計畫編號：DOH99-TD- N-111-003

行政院衛生署九十九年度科技研究計畫

超高靈敏度、無須標記且即時檢測腸病毒之奈米線場效電晶體生物感測器

研究報告

執行機構：國立交通大學

計畫主持人：楊裕雄

研究人員：賴文燦、蕭程允、林明瑜、林志衡、鄧康寧、林曉萍、蘇益志、陳雅辰、馮美惠、陳豪育、游智勝

執行期間： 99 年 3 月 1 日至 99 年 12 月 31 日

目錄

摘要：

關鍵詞：腸病毒；奈米線場效電晶體；半導體元件；生物感測器。

本計畫之目的為開發一套具有超高靈敏度、可即時多重偵測、操作簡便、並可結合台灣現有的半導體技術來大量生產的腸病毒奈米線場效電晶體生物感測器。實施方法為結合生物分子檢測技術及生物奈米半導體感測器，以腸病毒檢測與監控為標的，應用創新的矽奈米線場效電晶體生物分子感測及以積體電路設計之場效電晶體為基礎，開發分子檢測平台及監控系統。本年度計畫重點在於建立一新型量測系統，以提升腸病毒奈米線場效電晶體生物感測器訊號之穩定性。此量測方法應用 Lock-in detection 之原理，過濾雜訊，以導電性之變化取代電流量測。我們也同時開發了最佳奈米線場效電晶體之量測條件，應用 pH 值與導電值之變化決定閘極感測之最適電壓值，本研究部分成果發表於於國際期刊(Lu, M.-P., Hsiao, C.-Y., Lai, W.-T. and Yang, Y.-S. (2010) Probing the Sensitivity of Poly-Si Nanowire Field-Effect Transistors by Liquid-Gating pH Sensing, *Nanotechnology*, **21**, 425505. Featured as article "Liquid gate modulated nanosensors exhibit optimal sensitivity," on *Nanotechweb.org* (http://nanotechweb.org/cws/article/lab/44211)，並被選做專題報導。將特定腸病毒的 DNA 序列有專一性的單股 DNA 序列先固定在多晶矽奈米線場效電晶體表面，將互補和非互補的 DNA 序列流過奈米線場效電晶體表面，能對 DNA 序列作專一性辨識而兩互補的 DNA 序列產生雜交反應使奈米線場效電晶體的導電度產生變化，最低濃度可偵測到 fM (femto-molar,10^{-15}M)。此結果表示多晶矽奈米線場線電晶體具有高靈敏度、無需標誌且可即時偵測的潛能，此特性可發展成生物感測系統用來偵測腸病毒的感染型別並應用於其他傳染病篩檢。本感測方法具有可大幅改善未來腸病毒診斷的潛力，依目前研究成果與期中報告審查委員之建議，本計畫將以多晶矽奈米線場效電晶體元件與其與生物分子之作用為優先之研究方向。

Abstract

keywords：Enterovirus, Nanowire Field Effect Transistor, Semiconductor device, Biosensor.

The goal of this proposal is to develop an ultrahigh sensitive and easy to use biosensor for Enterovirus detection. Nanowire field effect transistor will be used as transducer for the biosensing device. In this research, polysilicon nanowire field-effect transistor (poly SiNWFET) was fabricated and functioned as a transducer for ultrasensitive, label-free and real-time detection of EV71. In previous year, we demonstrated its feasibility. We were focusing on the establishment of a new measurement system for poly SiNWFET to obtain a more stable electric signal. The electric noise was filtered based on theory of lock-in detection. The conductance was obtained following conversion from frequency signal. We also developed method to determine the optimal gate voltage for the biosensing experiment using variation of conductance at different pHs. Part of the results of this research was published (Lu, M.-P., Hsiao, C.-Y., Lai, W.-T. and Yang, Y.-S. (2010) Probing the Sensitivity of Poly-Si Nanowire Field-Effect Transistors by Liquid-Gating pH Sensing, *Nanotechnology*, **21**, 425505. Featured as article "Liquid gate modulated nanosensors exhibit optimal sensitivity," on *Nanotechweb.org* (http://nanotechweb.org/cws/article/lab/44211) and was selected as a featured article by the Nanotechnology journal. Specific single-strand DNA sequences that the unique DNA sequence of EV71 were immobilized on poly SiNWFET. Based on this new measuring scheme, the poly SiNWFET based EV71 biosensor exhibit a high sensitive and specific in respond to EV71. The functionalized poly SiNWFET and was stable in the presence of non-interacting ion molecules and was able to detect EV71 RNA at fM range. The results of this study suggest that the poly SiNWFET has a potential to be useful developed to a real-time, sensitive and label-free detection. The characteristics make it a potential biosensing system for early recognition that helps the treatment for EV71 infection. According to the recent progress and the recommendation from the review committee members, the future research will focus on the study on the poly SiNWFET and its responses to biomolecular interaction.

(1) 前言（包括研究問題之背景與現況、研究目的等）

研究問題之背景與現況

腸病毒病原分佈廣泛且生存力強(Tables 1-4, Figures 1-3)可在環境中長久存活，在溫帶氣候地區，腸病毒通常流行於夏季，而台灣地處亞熱帶，流行的季節性不明顯，全年皆可能有感染個案發生。腸病毒傳染途徑多元，且患者可釋出病毒長達8-12週，病毒傳染力極強，藉由飛沫傳染、糞口傳播及接觸病人分泌物等受到感染，潛伏期2-10天，平均3-5天，但在發病前數天，喉嚨及糞便都有病毒存在，在發病後一週內傳染力最高，患者可從腸道內持續釋出病毒長達8-12週。即時的腸病毒診斷方法，為預防與治療腸病毒感染最佳之工具。

目前腸病毒診斷的困難有：1. 無症狀或似感冒症狀佔多數，醫師經驗不足，皆容易導致誤診，造成不自覺傳播。受到腸病毒感染後，約有50-80%的人不會發病，或只有類似一般感冒的輕微症狀，造成不自覺傳播，如果將病毒傳播給面議系統尚未發展成熟的嬰幼童或免疫力低下者，造成重度併發症，且台灣地狹人稠、交通方便，很容易造成全面流行。2. 部分臨床醫師對於腸病毒感染併發重症病徵認知不足，錯失治療最佳時機。腸病毒感染併發重症，最重早期診斷，早期治療，部份臨床醫師因經驗不足，對重症病徵認知不足，將影響醫護品質。3. 臨床確立診斷時間過長。因現有診斷方式限制，當有疑似病徵出現，病患檢體送檢，至少需要4天以上，可能因為診斷時間過長及不便利性，會造成家長或患者不願花錢住院或等待，無法確定病因，而忽略併發重症的嚴重性或是不自覺傳給其他免疫力低下的嬰幼童，造成傳染範圍擴大，及無法預期的嚴重後果。4. 臨床檢體採集限制多，會影響到診斷可信度及增加社會成本的支出。。根據疾管局的防疫檢體採檢手冊，不同的檢體種類和採檢目的會有不同的適合的採檢時機，也因為無法即時檢測，所以檢體需要加肝素 (Heparin)以防凝血、低溫運送到檢測單位，造成檢體採集限制多，增加社會成本的支出，如果未在規範內將檢體送檢，可能會影響到診斷可信度，所以有待改進檢體採集診斷之方法。

不論是現有臨床檢驗方式或是新式腸病毒檢驗方法，其最大缺點就是花費時間長，無法立即偵測，影響到診斷時間及治療契機，所以發展一套即時的腸病毒檢驗裝置實在刻不容緩。

研究目的

本計畫目標為應用創新的矽奈米線場效電晶體生物分子感測平台開發適用於腸病毒檢測與監控的即時檢驗裝置。同時以生醫應用為導向，整合積體電路設計與儀器開發技術，發展分子檢測平台及監控系統，發展未來生醫電子晶片產品。研究重點為結合半導體製程、生物分子檢測技術、儀器開發技術、臨床檢測技術，開發一套具有超高靈敏度、可即時多重偵測、操作簡便、並可結合台灣現有的半導體產業來大量生產的奈米線場效電晶體腸病毒生物感測器。依目前研究成果與期中報告審查委員之建議，本計畫將以多晶矽奈米線場效電晶體元件與其與生物分子之作用為優先之研究方向。

(2) 材料與方法

2-1 *Experimental material*

1. 3-Aminopropyltriethoxysilane (APTES): $H_2N(CH_2)3Si(OC_2H_5)_3$
   Company: Sigma-Aldrich (USA) (A3648)
   CAS Number : 919-30-2
   Assay: ≥98%
2. Sodium cyanoborohydride: $NaBH_3CN$
   Company: Sigma-Aldrich (USA) (71435)
   CAS Number : 25895-60-7
   Assay: ≥95% (RT)
3. Ethanolamine hydrochloride: $NH_2CH_2CH_2OH \cdot HCl$
   Company: Sigma-Aldrich (USA) (E6133)
   CAS Number : 2002-24-6
   Assay: ≥99
4. Glutaraldehyde solution: $OHC(CH_2)_3CHO$
   Company: Fluka (USA)
   CAS Number : 111-30-8
   Grade: technical
   Concentration: ~25% in H_2O (2.6M)
5. Potassium phosphate monobasic: KH_2PO_4
   Company: J.T.Baker (USA)
6. potassium phosphate dibasic: K_2HPO_4
   Company: J.T.Baker (USA)
7. Ethanol (99.5%): CH_3CH_2OH
   Company: Echo Chemical Co. (Taiwain)
8. Polydimethylsiloxane (PDMS): $(H_3C)_3SiO[Si(CH_3)_2O]_nSi(CH_3)_3$
   Company: Sil-More (Taiwan)
9. EV71 DNA sequences were designed for capture probe and the target DNA used on this project are listed as below and based on previous publication [27]. All synthetic oligonucleotides were purchased from MDBio Inc. (Taiwan).
   5'-amino C_6 modified captured DNA probe

	DNA sequences (5'-3')	
	5'-H_2N C_6 modified captured DNA probe	Target DNA
EV71 [a]	GTG GCA GAT GTG ATT GAG AG	CTC TCA ATC ACA TCT GCC AC
CA16 [b]	GAG TGA TGG TTC AAC ACA CA	TGT GTG TTG AAC CAT CAC TC

[a] relative to BrCr nt 2448-2467

[b] relative to G-10 nt 2666-2685

10. Phosphate buffer solution (PBS) was prepared by Potassium phosphate monobasic and Potassium phosphate dibasic dissolved in de-ionized water at 10 mM, adjusting pH value by buffer titration.

11. Deionized water (DIW)
resistance of water: 18.2 MΩcm
ultra-pure water system (Barnstead).

2-2 *Instruments*

The whole instrument consisted of electrical measurement machine (Dual-channel System Source Meter Instrument Model 2636) (Keithley), probe station with its chamber (EVERBEING(奕葉)), and programming syringe pump (Kd Scientic) (Figure 4).

2-3 *Poly crystalline silicon NWFET fabrication process*

First, the fabrication began on Si wafers capped with a 100 nm-thick thermal oxide. The second, a 50nm-thick nitride layer was deposited by low-pressure chemical vapor deposition (LPCVD). After deposition of the nitride layer, following deposing Tetraethyl ortho-silicate (TEOS) 100nm thick sketched with standard photolithographic and etching steps were performed to form the oxide dummy structures. Subsequently, a 100nm-thick amorphous-Si layer was deposited and then annealed at 600°C for 24hr in N_2 ambient to transform it into polycrystalline structure. Afterwards, source/drain (S/D) doping was done with phosphorus ion implantation with a dose of $5E^{15}cm^2$. After the generation of S/D photoresist patterns with a lithographic step, a reactive plasma etching step was performed to form the S/D regions. Because of the anisotropic etching process, two poly-Si NW channels were formed separating by oxide dummy gate simultaneously during the S/D etching step.

By carefully controlling the etching time, the cross-sectional dimensions of poly-Si NW channels can be easily reduced to sub-10 nm scale. Subsequently, all devices were then covered with a 200nm-thick TEOS oxide passivation layer. Finally, remove the oxide layer by 2-step dry/wet etching process to expose the poly-Si NW channels.

2-4 *Microfluidic system*

The microfluidic channel system was made with acrylic, PDMS and metal holder. First, the PDMS gel was covered to the channel patterned glass substrate (channel size: 13 mm X 1 mm X 0.5 mm) at 120°C for 10 minutes and wait for the fluid gel transfer to solid state. The solidification PDMS channel was separated from the glass substrate and covered to the SNW chip. Then, make the limpid acrylic blanket and drill two holes filling with Teflon tubes (outer diameter: 1.5 mm, inner diameter: 0.5mm) for sample transport. Finally, limpid blanket of acrylic was covered to the PDMS and the chip-PDMS-acrylic sandwich was fastened by a metal holder. The advantage of the microfluidic channel system is easy alignment, easy observation and be reused. The schematic diagram of the microfluidic system is shown in Figure 5.

2-5 *Surface modification*

We would do some treatments on chip surface before we measure the electrical variation. The immobilization process is based on the microfluidic system. Initially, we aligned the PDMS microfluidic channel covered on nanowire device row and added acrylic blanket on PDMS solid gel. Then, fastened the blanket and PDMS gel on nanowire chip by metal holder like the sandwich structure, tested whether the fluid buffer seep from the sandwich-stacking microfluidic system (Figure 5). After setting up the microfluidic system, it shall be locked an injection tubing connector. Inject APTES in ethanol solution 1 ml through microfluidic channel and react for 17~20 minutes. Then, wash the channel with 95% ethanol. Turn on hot plate and set the temperature about 110℃~120℃, put the whole microfluidic system on the hot plate for 10 minutes. Then, cool the metal holder to room temperature and inject 2.5% glutaraldehyde reacting for one and half hour in 10 mM pH 7 phosphate buffer. Nanowire surface functional group would be changed from hydroxide into aldehyde group, we would use DNA sequence modified amino-C6 at 5' end as a DNA probe to bind with surface aldehyde. A 20-mer DNA sequence was diluted in 10mM pH 7 phosphate buffer, injecting 1 μM to microfluidic channel for 3 hours or more. Continuously, block unbinding aldehyde group with 50 mM ethanolamine at pH 9.1

phosphate buffer for one and half hour. Finally, wash the channel with pH 7 phosphate buffer and ready measure. The overall surface modification is shown in Figure 6.

2-6 *Sample transport at kinetic equilibrium*

In order to maintain the environment ionic strength level, we keep the microfluidic channel fluent to replace of quiescent state. First, set the microfluidic system connecting a syringe pump at injection end and be locked a liquid gate at the elution end. The waste buffer shunted by T-shaped tubing (Figure 7), sealed the end of metal wire by silicone neutral sealant. Then, fix the flow velocity at 5 ml/h by Syringe Pump (Kd Science) (Figure 8). Sample will be exchanged by changing another syringe tube, a little bubble between two solution samples. The whole transport system is semi-automatic, which fixed flow velocity by machine but changed syringe tubes by people.

2-7 *Liquid phase electrical measurement*

It has been reported that the electrical properties would be different from air to liquid phase environment. We would immobilize chemical compounds and biomaterials on nanowire chip in microfluidic channel for 6 hours, changed surface functional group in liquid phase. After treating the chip for a long time, we measured the device properties by conductance-time method, compared with those relations of the shift of threshold voltage to air condition and its' stability. We measured these data and calculated mathematically signal process, found the most sensitivity Vg point. We got a plot for describing the relationship of conductance-Vg (liquid gate) and a voltage which has the most sensitive variation rate. Then, fixed the Vg and measured pH sensing to check correcting variation trend.

(3) 結果 與 (4) 討論

3-1 *Nanowire chip selection in dry air condition*

Nanowire Field Effect Transistor (NWFET) wafers were fabricated at Class 100 clean room of National Nano Device Laboratory (Hsinchu city, Taiwan, R. O. C.), sealing in an anti-electrostatic bag. We need to check the electrical properties before biosensing, by using electrical analysis machine (Keithley 2636) to measure NWFET chips. For the purpose, one standard operation process was built (Figure 9) to screen good chips, record the data of Id-Vg plot and key parameters of threshold voltage, on/off current ratio (Figure 10-A& 10-B), and then, look for good and stable chips for biosensing. Chip selection principles were defined in Table 6, classified into three ranks, best, acceptable and failed.

3-2 *Biosensing of non-immobilized semiconductor device*

Initially, the control set of conductance measurement was calculated by measuring the electrical variation of bare chip. The real-time changeable conductance was observing in all experimental preparation setup. First, the microfluidic channel was filled with 10 mM pH 7 phosphate buffers and kept the buffer flowing. The conductance value won't change too much if we don't do any action. When the syringe tube was changed, a big pulse wave appeared, caused by the little bubble between two buffer solutions. These results show it didn't change obviously because we just change the same solution to test whether the device is stable after the bubble pass through. Then, we injected 100 pM CA 16, the signal didn't change obviously after the bubble peak passed because of no immobilization on nanowire device. After CA 16 DNA sample was injected, washed the microfluidic channel by pH 7 buffer before next sample. Then, we switched EV 71 DNA sample, the signal still be kept in baseline. Finally, we washed the channel by pH 7 buffer solution to clean the microfluidic channel, the signal still be kept in baseline at last. Those overall results show that the conductance electrical signal won't change obviously without functionalizing nanowire device surface (Figure 11).

3-3 *Device characteristic verification in liquid phase*

After surface modification on NWFET chips, and the electrical characteristic of the device was tested. We want to know two main goals that the variation trend of the most sensitive voltage point is also based on the sensing theory. First, we swept the liquid gate voltage to check the electrical variation controlled by liquid and calculate

these data. The conductance value (red line) (Figure 12) will be increased as liquid gate is increased and fitted the N-type device features. Then, differentiate the conductance value with liquid gate values to get G_m values. Finally, G_m values are divided by conductance values (G) to get sensitivity values (Sensitivity=G_m / G , G_m = dG / dV). After those mathematic operations, we got the Vg value with maximum variation rate at sub-threshold region. Both biosensing and pH sensing shall be operated at fixed Vg value we calculated before. On the other side, we would check whether the variation trend of the conductance signals fitted its doping type. In this experiment, we applied N-type NWFET as sensing device, to observe the signal changeably fitting N-type characteristic. When the buffer switched from pH 7 to pH 8, it will have more negative ion than pH 7, to make N-type NWFET induced less electrons passing through those channels. Reversibly, buffer solution switched from pH 8 to pH 7, it has less negative ion than pH 8, to make N-type NWFET inducing more electrons pass through those channels. The conductance value is directly relative to the current of nanowire channels. As the results are shown in Figure 13, the conductance value could reversibly change from different pH buffers fitting N-type device characteristic.

3-4 *Enterovirus 71 (EV 71) DNA Biosensing*

After surface functional group modification and reaction with EV 71 DNA probes (Shown as Figure 6), we measured the real-time conductance signals of injecting buffer or samples in fixed flow rate by syringe pump (Kd Science). In the experiment, the probe DNA was designed 20 base long and amino hexyl was modified at 5'-end with complementary DNA strand as target DNA but no modified at both ends.

In addition, we design a CA16 as a negative control to confirm the probe DNA of specifically binding to its' complementary DNA. All samples were diluted by phosphate buffer (10 mM, pH 7.0) and we regard the buffer condition as baseline in the experiment. First, we would make a bubble to generate a signal pulse observing whether the baseline shift or not. So as to the other pulses when we switching to another samples, the bubble means to signal income. Second, it will be injected 10000 times concentration negative control (CA 16) than positive sample (EV 71) to observe whether the signal variation, then eluting the CA 16 with phosphate buffer. Third, inject the EV 71 1 fM into the channel to react with probe DNA. We can see those conductance value of 1 fM EV 71 obviously changed than 100 pM CA 16 as shown in Figure 14. Finally, we added 100 fM EV71 to check whether the reaction saturated,

compared with those conductance changed percents among control and experiment data (Figure 15). As these results, the real-time conductance analysis method can specifically identify both complementary DNA and non-complementary DNA. The proposed measuring system has advantages like label-free, real-time and high sensitivity. It's promising to develop semiconductor biosensor.

3-5 *EV 71 DNA biosensing after hot water washed*

After the EV 71 biosensing, we injected 10~15ml hot water (over 80 ℃) to remove the hybridized DNA sequence (T_m: 51.8 ℃). Then, washed the microfluidic channel by phosphate buffer (room temperature) and repeated previous process again. First, we would sweep liquid gate to observe the conductance value still controlled by liquid gate because we didn't know how the hot water affected the device characteristic. Secondly, got those data of conductance to liquid gate and calculate the most sensitivity Vg point. Compared to Figure 9, the most sensitive Vg point shifted to 1.65 V (Figure 16). We considered that (1) the device was decayed since the first biosensing process (2) after the hot water washed the device surface suffered damage. However, we followed up previous process to do biosensing again. In the beginning, the baseline was rised up continuously, even we injected CA 16 (control set) DNA sample. But the conductance value will be decreased obviously when EV 71 (experiment set) injected. We got the same response even though the baseline was not as flat as these previous results. We can say that the conductance signal could truly reflected bio-reaction on device surface (Figure 17).

3-6 *CA 16 DNA Biosensing*

In contrast to EV 71 biosensing, we do another experiment by immobilizing CA16 DNA probe and detecting complementary CA 16 target sequence. The EV 71 DNA strand became control set in the experimental design. According to the same previous process to sweep the Vg, the most sensitive Vg point was calculated as shown in Figure 18. We got the Vg value about 1.03 V and started biosensing by the fixed Vg value. In the beginning of CA 16 biosensing, we injected 100 pM EV 71 DNA sample as control set, and the conductance value still be kept on baseline. Then, injected 1fM CA 16 and the conductance value didn't shift obviously. As injected 100 fM CA 16, the conductance value shifted down slowly. A little difference from EV 71 biosensing results, the conductance value would rise when we injected pH 7 PBS buffer to wash the channel. Similarly, we injected higher concentration of CA 16. It

can obtain more variation than lower concentration samples, but still be recovered when buffer injected (Figure 19). After biosensing, we compared those different concentrations of CA 16 samples and control set (Figure 20), it was revealed the variation rate directly proportional to concentration. Finally, we proposed that the reason of the conductance value reversed when buffer injected. The distortion of microfluidic PDMS may change the streaming potential, to cause the hybridized DNA flushed by buffer. The higher concentration of CA 16 samples still reacted with immobilized DNA probes. It performed high specificity of biosensing because it didn't react with control set.

(5) 結論

In our research, we have demonstrated the poly crystalline silicon NWFET could be developed as a highly sensitive, specific and label-free biosensor to detect EV71 and CA16 nucleic acid in a real-time kinetic measurement system. The device yield is not yet as good as commercial products, we still provide a standard operation process to pick up good device for biosensing. By the lock-in detection and sample transport system, we could filter out a lot of noise to extract conductance signal. It helped us measuring bio-reaction at steady state. Not only apply on rapid diagnosis but also be suitable to investigate the molecular bio-reaction. Furthermore, the poly crystalline silicon NWFET fabrication process is compatible to modern semiconductor technology in Taiwan. It could be mass production for many applications. Therefore, the poly crystalline silicon NWFET could provide a great potential for real-time, label-free and highly sensitive molecular diagnostics or other scientific applications (Table 7).

(6) 計畫重要研究成果（本項目請用中文書寫）

1.本計畫之重要成果

1. 目前多晶矽奈米線場效電晶體元件，已經依正常下單程序由國家奈米元件實驗室之元件流程定期穩定製備。我們已建立起晶片篩選系統，在尚未商業化前，可以有效的選出可以應用於生物感測之元件。若可以找到合作的半導體廠商，應用我們已開發的製程將可以大量且高良率生產多晶矽奈米線場效電晶體元件。
2. 檢測腸病毒之矽奈米線場效電晶體原型機構形設計及製作已初步完成(與國家實驗研究院儀器科技研究中心合作)。
3. 會議及期刊論文發表 (DOH99-TD-N-111-003)
   1. Yang, Y.-S. (2010) Biochemical Electronics in a Synthetic-Bio Hybrid System: The Future Bio-Electronic Device, 2010 Symposium on Nano Device Technology (SNDT 2010), May 4-5, Hsinchu, Taiwan (Invited Talk).
   2. Yang, Y.-S. (2010) Poly Crystalline Silicon Nanowire Field-Effect Transistor Based Biosensors, International Conference on Cellular & Molecular Bioengineering (ICCMB), August 2-4, Singapore (Oral Presentation).
   3. Hsiao, C-Y., Lai, W.-T., Lu, M.-P. and Yang, Y.-S. (2010) Poly Crystalline Silicon Nanowire Field-Effect Transistor for Real-Time Detection of Influenza Virus DNA, 2010 International Conference on Solid State Devices and Materials (SSDM 2010), September 22-24, Tokyo, Japan (Oral Presentation).
   4. C.-C. Hsu, Lu, L.-Y. and *Yang, Y.-S. (2010) From Sequence and Structure of Sulfotransferases and Dihydropyrimidinases to an Understanding of Their Mechanisms of Action and Function, *Expert Opinion on Drug Metabolism & Toxicology,* 6, 591-601.
   5. Lu, L.-Y., Hsu, Y.-C. and *Yang, Y.-S. (2010) Spectrofluorometric Assay Monoamine-preferring Phenol Sulfotransferase (SULT1A3), *Analytical Biochemistry*, **404**, 241-243.
   6. Lu, M.-P., Hsiao, C.-Y., Lai, W.-T. and *Yang, Y.-S. (2010) Probing the Sensitivity of Poly-Si Nanowire Field-Effect Transistors by Liquid-Gating pH Sensing, *Nanotechnology*, **21**, 425505. Featured as article "Liquid gate modulated nanosensors exhibit optimal sensitivity," on *Nanotechweb.org* (http://nanotechweb.org/cws/article/lab/44211)

2.本計畫之重大突破

1. 由於其突破性的效率與在生醫感測上的應用，以奈米線場效電晶體為感測元件之研究在國際間備受重視。若以其產業價值衡量，目前唯有由本團隊研發製備之多晶矽奈米線場效電晶體，不但已證實為優良的生醫半導體元件，並且可以以低成本，運用商業化製程大量生產，因此本研究已具相當優勢。加上台灣半導體產業之實力，以產品開發的目標而言，我們更具有國際競爭力。
2. 本研究(與國家實驗研究院儀器科技研究中心合作)第一個將奈米線場效電晶體整合成檢測腸病毒之原型機。
3. 本研究的腸病毒檢測方法，為目前已知最靈敏且可立即偵測的方法。

(7) 主要成就及成果之價值與貢獻度（本項目請用中文書寫）

人類壽命逐年增加，威脅人類的疾病種類雖然有所變化卻始終不曾間斷，慢性疾病及預防醫學已成為現代與未來醫療的主軸。各種疾病之早期診斷與即時監控，為能長期維持優質生活之關鍵，因此需發展高專一性、高靈敏度且快速之定點或個人化之生醫感測系統，這是醫療檢測上的一大挑戰與商機。我們已成功的開發出可用標準半導體製程製作的多晶矽奈米線場效電晶體，可達到大量生產的目標，且藉由腸病毒生物感測，驗証其在生物感測的實用性。相信此一研究的成功在未來的醫療感測上將會帶來莫大的幫助，並可開創台灣新興的生物科技與半導體產業。

(8) 參考文獻：

1. 行政院衛生署疾病管制局. "*腸病毒感染併發重症(含非小兒麻痺病毒之腸病毒感染症)*", 2007, [cited; Available from: http://www.cdc.gov.tw/index_info_info.asp?data_id=1007.
2. Huang, K.Y. and Lin, T.Y. "*Enterovirus 71 infection and prevention*", *Taiwan Epidemiology Bulletin*, 2008, p. 415-426
3. Lin T.Y. et al. "*The 1998 enterovirus 71 outbreak in Taiwan: Pathogenesis and management*", *Clinical Infectious Diseases*, 2002, 34, p. S52-S57.
4. King, A.M. et al. "*Family Picornaviridae. In Virus Taxonomy.*, in *Seventh Report of the International Committee on Taxonomy of Viruses*", *San Diego: Academic Press.*, 2000, p. 657-678.
5. Lin, T.Y. et al. "*Enterovirus 71 outbreaks, Taiwan: occurrence and recognition*", *Emerging Infectious Diseases*, 2003, 9(3): p. 291-293.
6. Wang, S.F. "*An epidemiological analysis of enterovirus 71: Taiwan, 1998-2004*", *Taiwan Epidemiology Bulletin*, 2005, p. 125-153.
7. Wu, H.S. et al. "*Update on the Molecular Epidemiology of Human Enterovirus 71 in Taiwan Since 1998*", *International Journal of Infectious Diseases*, 2008, Vol. 12 (Supplement 1).
8. Chang, L.Y. et al. "*Comparison of enterovirus 71 and coxsackie-virus A16 clinical illnesses during the Taiwan enterovirus epidemic, 1998*", *The pediatric infectious disease journal*, 1999, 18(12): p. 1092-1096.
9. 行政院衛生署疾病管制局 "*腸病毒感染併發重症臨床處理注意事項*", 2010.
10. 行政院衛生署疾病管制局 "*傳染病防治工作手冊-腸病毒感染併發重症*", 2008.
11. 行政院衛生署疾病管制局 "*腸病毒感染防治手冊*", 2007.

(9) 圖、表

Table 1

Enterovirus were classified based on their genomic sequences

Classified	Serotypes
Human enterovirus A (HEV-A)	Coxsackie virus A2-8, 10, 12, 14, 16 Enterovirus 71, 76, 89-92
Human enterovirus B (HEV-B)	Coxsackie virus A9 Coxsackie virus B1-6 Echovirus 1-7, 9, 11-21, 24-27, 29-33 Enterovirus 69, 73-75, 77-88, 93, 97-98, 100-101
Human enterovirus C (HEV-C)	Coxsackie virus A1, 11(15), 13(18), 17, 19-22, 24 Enterovirus 95-96, 99, 102 Poliovirus 1-3
Human enterovirus D (HEV-D)	Enterovirus 68, 70, 94
New (unclassified)	

Table 2

The common disease related enterovirus serotypes[11].

Common diseases	Virus serotype
hand-foot-mouth disease (HFMD)	Coxsackievirus group A16 (CA16), CA4, 5, 9, 10, CB2, 5, EV71
Herpangina	CA 1-10, CA16, CA22, EV71
Pleurodynia	Coxsackievirus group B (CB)
Acute myocarditis and pericarditis	CB
Acute meningitis and encephalitis	CA10
Aseptic meningitis and encephalitis	Coxsackievirus, poliovirus, echovirus, EV71
Febrile illness with rash	Coxsackievirus, echovirus

Table 3

Proposed pathogenesis of severe Enterovirus 71 infections [3]

Stage	Syndrome	Underlying cause
1	Hand-foot-and-mouth disease (HFMD)/ herpangina	-
2	Encephalomyelitis	Direct invasion or viremia
3	Cardiopulmonary failure A: Hypertension B: Hypotension	Neurogenic inflammatory response
4	Convalescence	-

Table 4

Historical perspective and case incidences of Enterovirus 71 in worldwide.

Year	Description
1969	First isolated in California
1972	Melbourne, Australia
1974	Sweden
1973	Japan
1975	Bulgaria with 44 deaths
1978	Hungary with 45 deaths
	Japan
1985	Hong Kong
1986	Nan-ao, Taiwan
1997	Malaysia with at least 30 deaths
1998	Taiwan with 78 deaths
2000	Taiwan with 25 deaths
2001	Taiwan with 26 deaths

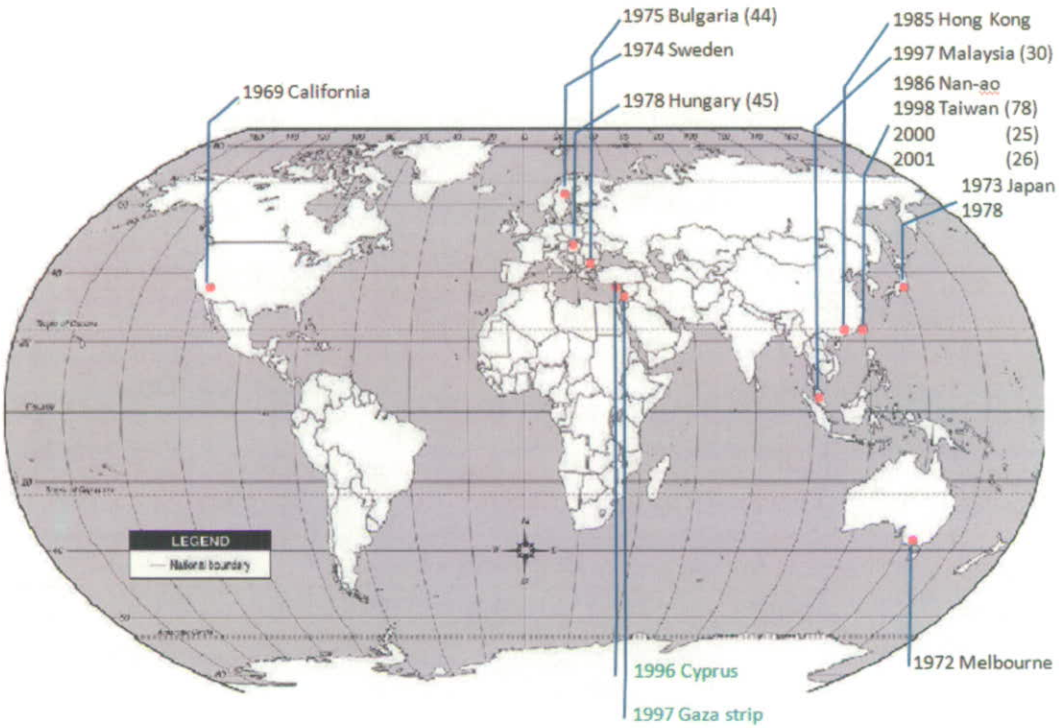

Figure 1 The epidemiology of enterovirus around the world, since 1969.

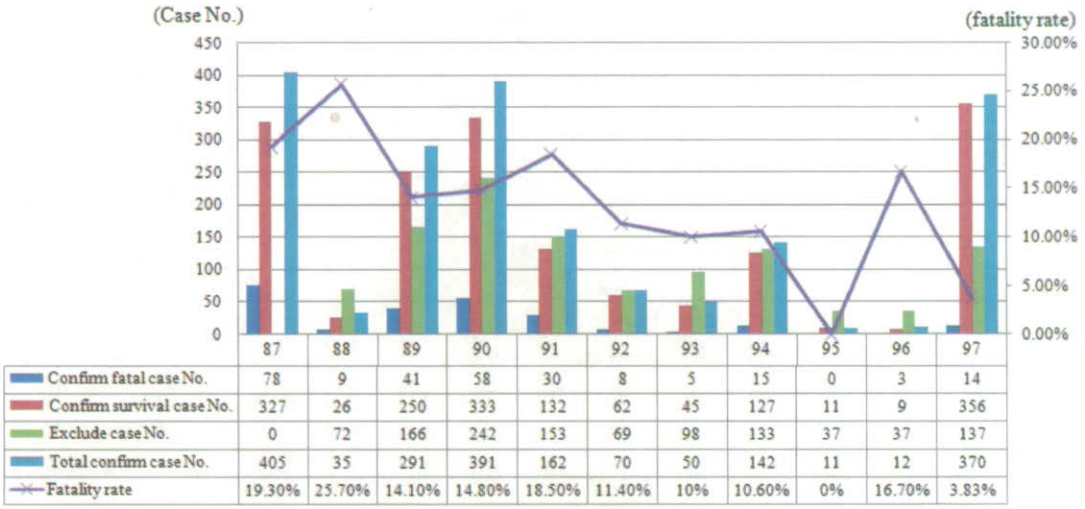

	87	88	89	90	91	92	93	94	95	96	97
Confirm fatal case No.	78	9	41	58	30	8	5	15	0	3	14
Confirm survival case No.	327	26	250	333	132	62	45	127	11	9	356
Exclude case No.	0	72	166	242	153	69	98	133	37	37	137
Total confirm case No.	405	35	291	391	162	70	50	142	11	12	370
Fatality rate	19.30%	25.70%	14.10%	14.80%	18.50%	11.40%	10%	10.60%	0%	16.70%	3.83%

Figure 2 Epidemic situation of Enterovirus infection with severe complications in Taiwan, 1998-2008. (redraw from CDC, 疫情報導 676, 938)

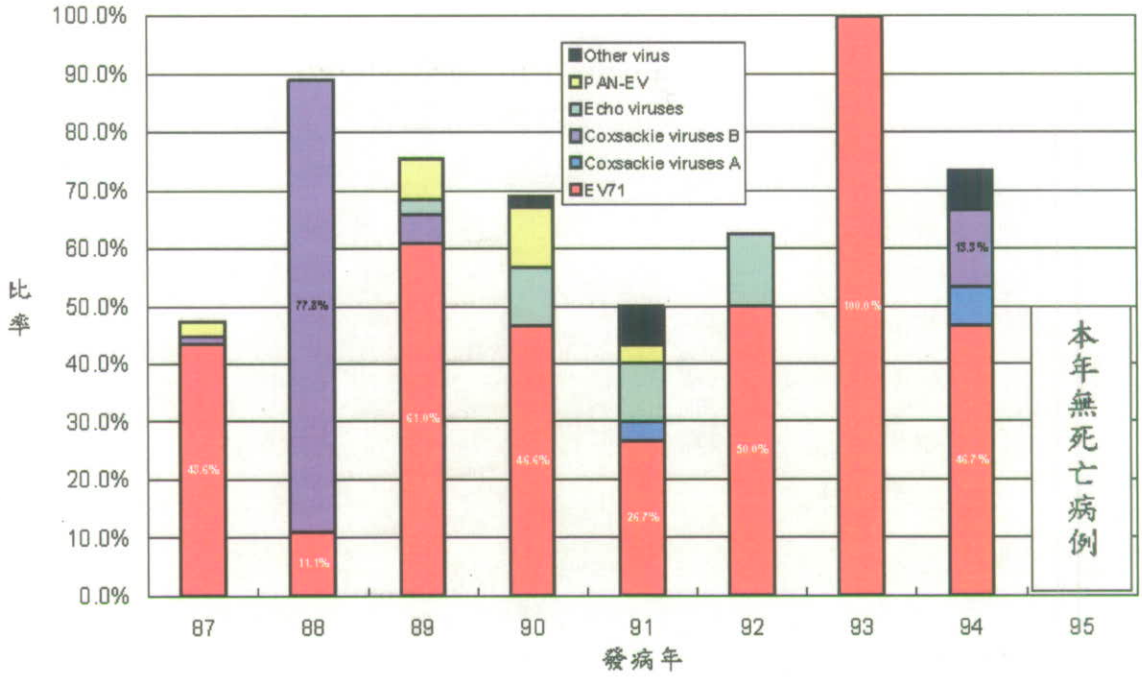

Figure 3 The distribution of serotypes of virus isolation from severe fatal case, 1998~2006 [11]

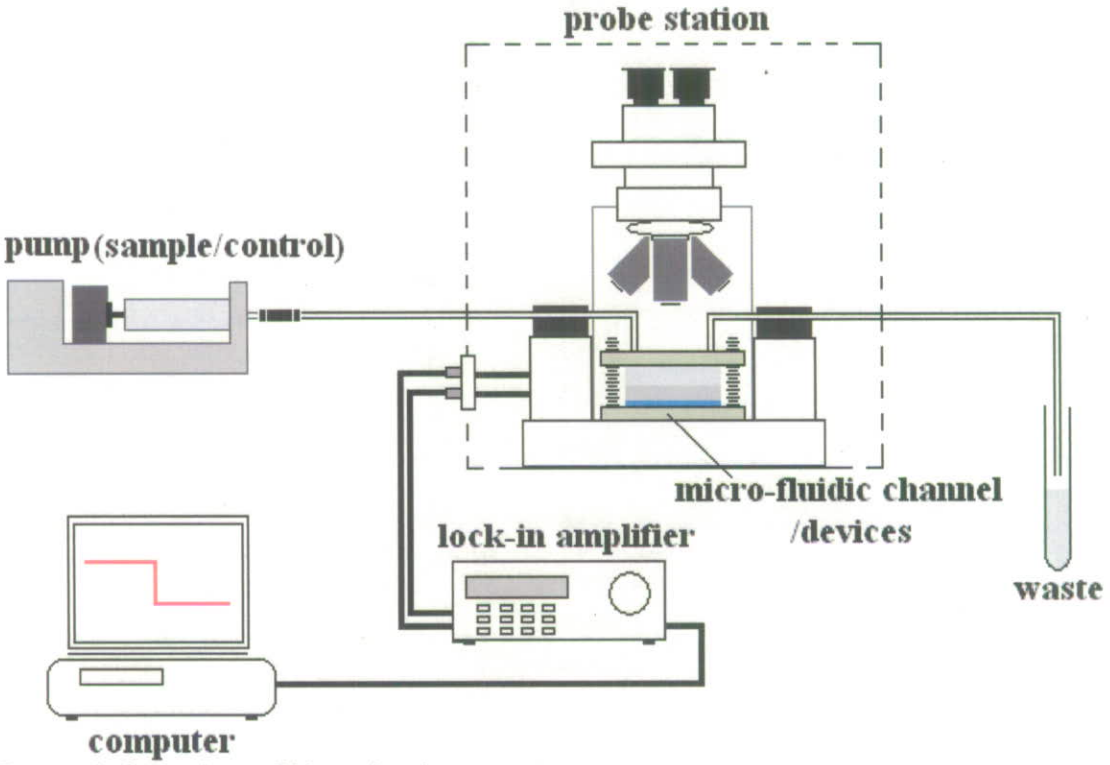

Figure 4 Overview of biosesing instruments.

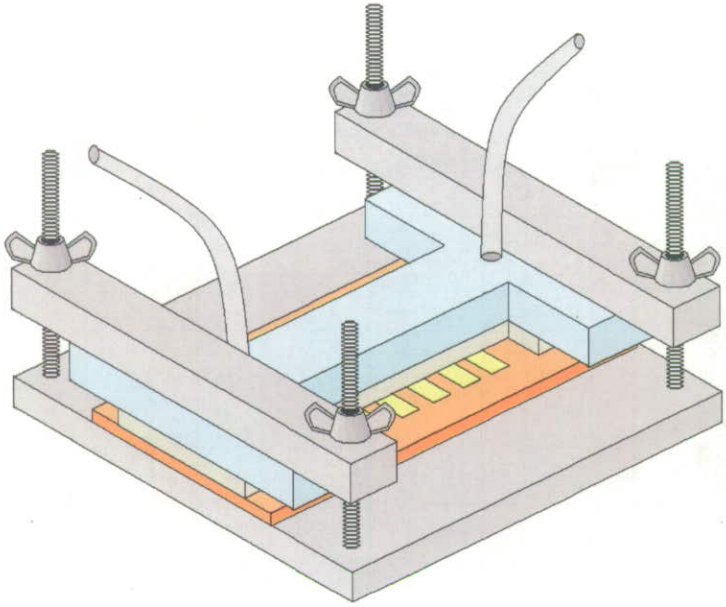

Figure 5 Schematic diagram of microfluidic channel for the biosensing with Si NW FET

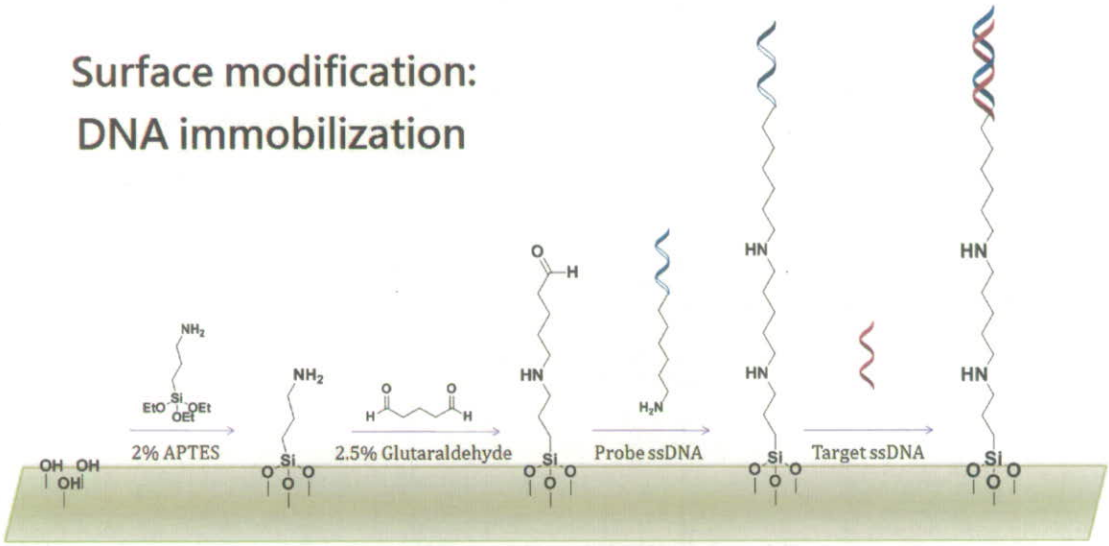

Figure 6 DNA immobilization process in microfluidic system

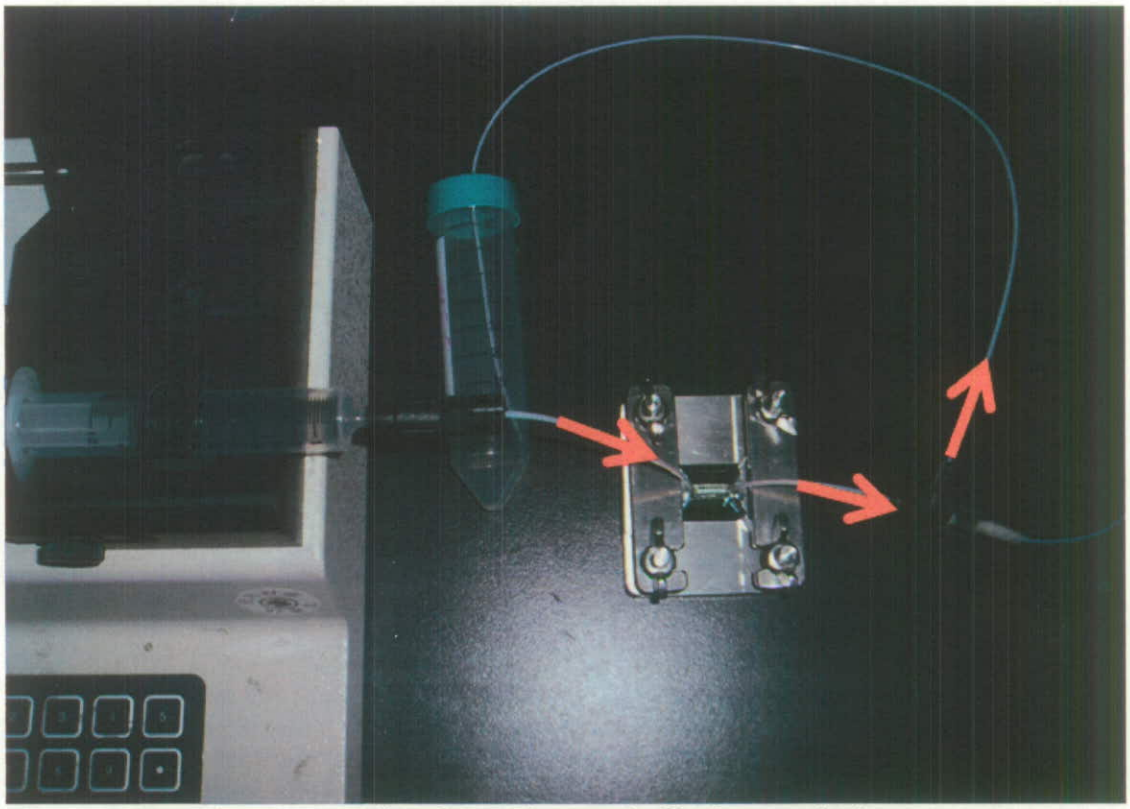

Figure 7 Sample transport direction and waste buffer bypass device

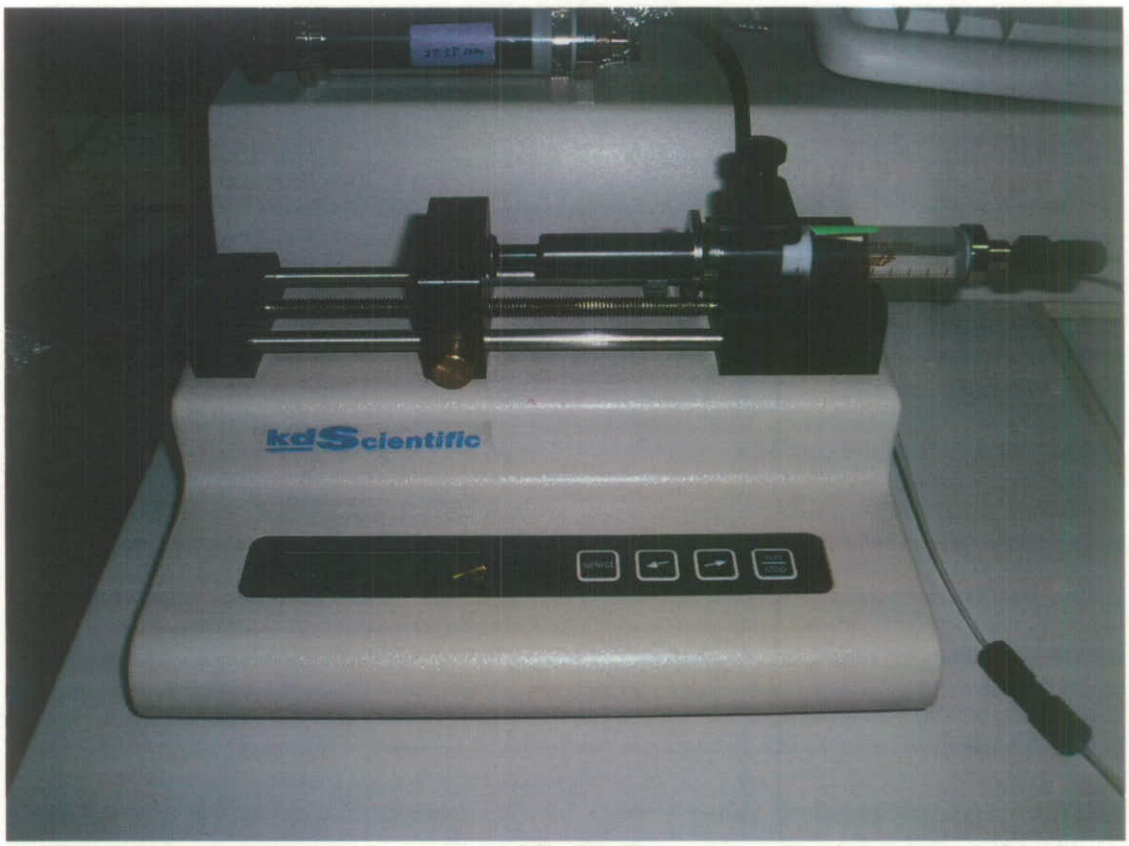

Figure 8 Programming Syringe pump (Fix the flow rate and volume by machine)

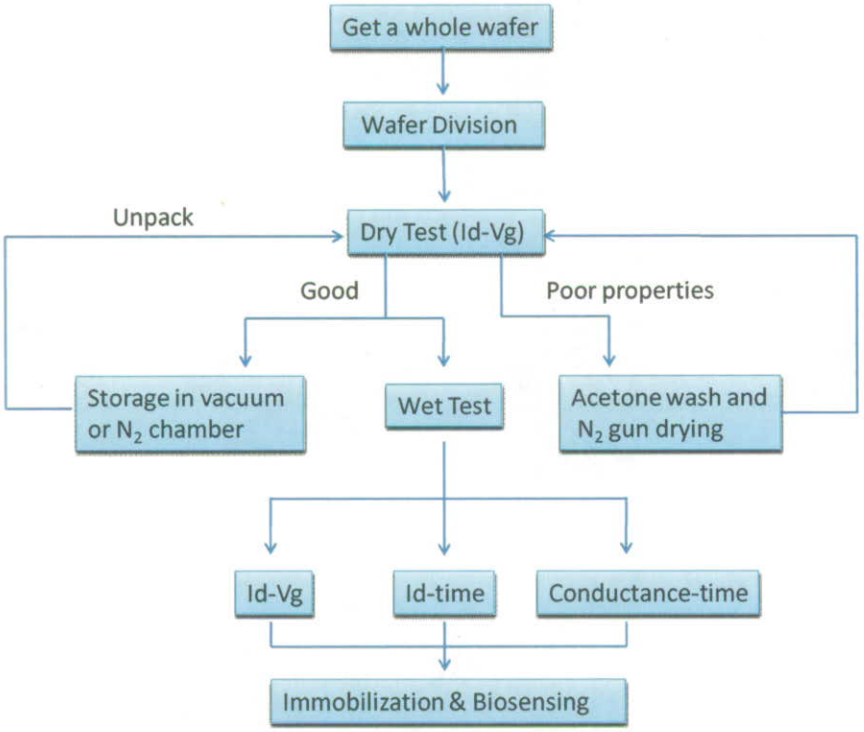

Figure 9 Standard operation process of device selection in dry air

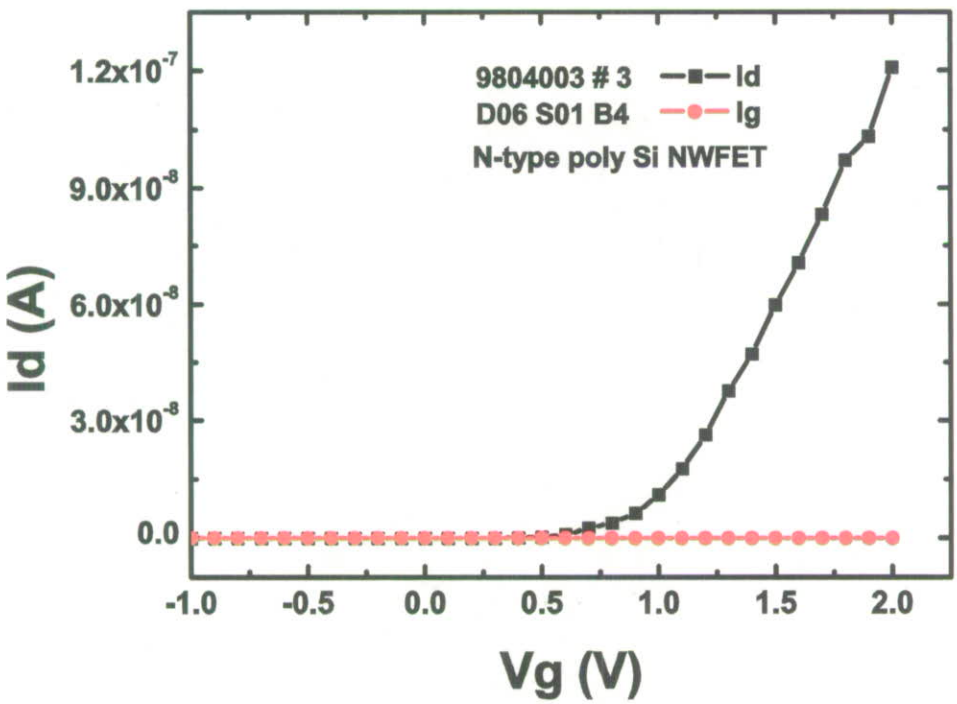

Figure 10-A N-type poly-Si NWFET measurement in dry air Vsd= 0.5V , Vgd sweep from -1V to 2V, threshold voltage ~ 1.0V .

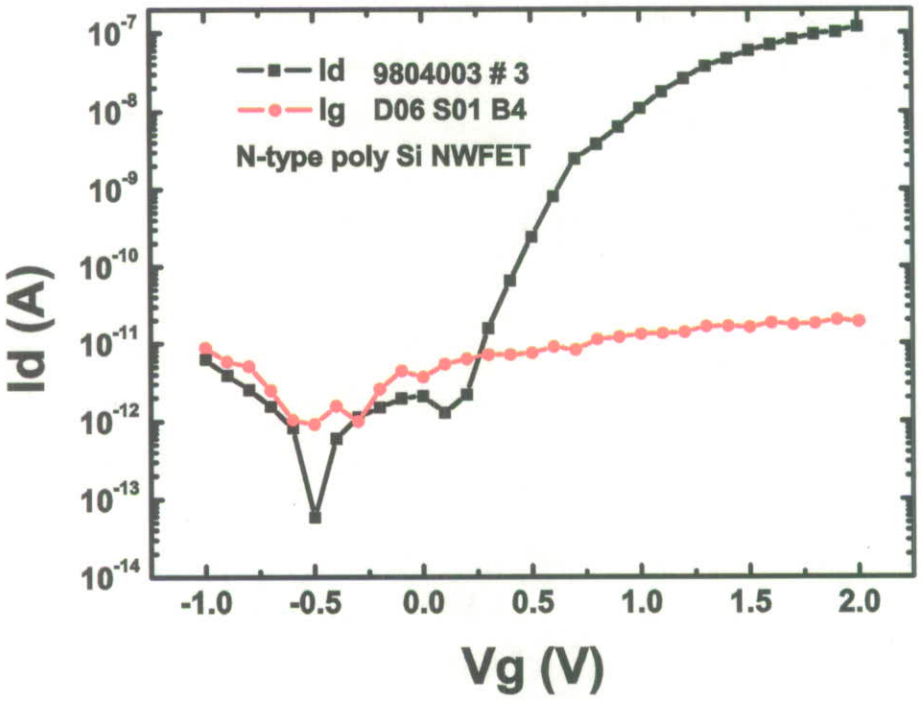

Figure 10-B The same data as Fig. 1A but in form of log scale plot. Its' drain current Id from 10^{-12} A to 10^{-7}A, leakage current Ig~10^{-12}A , on/off ratio~10^{5} .

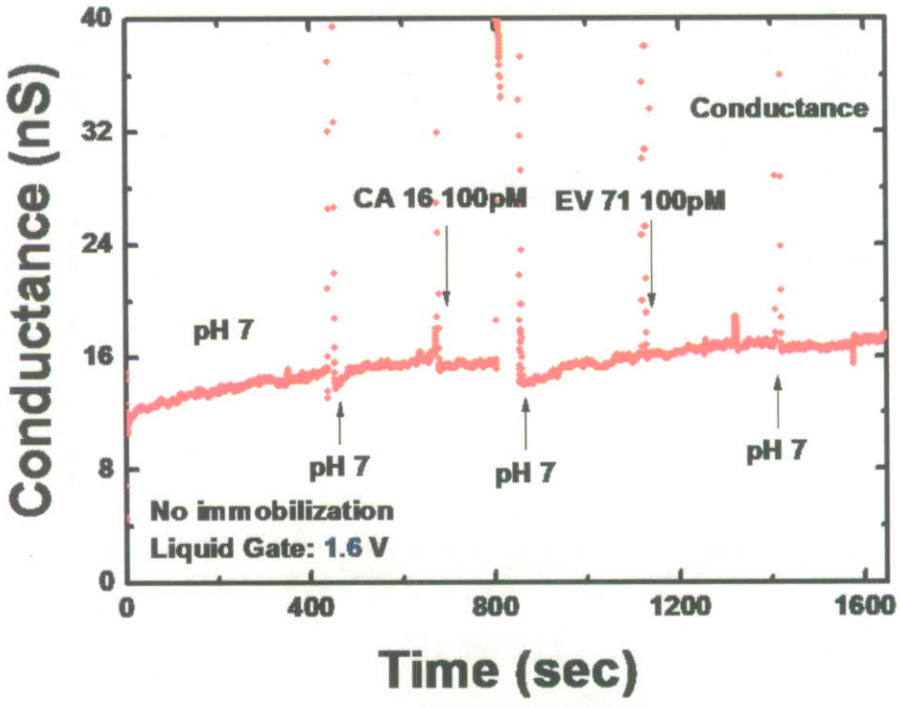

Figure 11 Without any immobilization process, this biosensing acts as a control set.

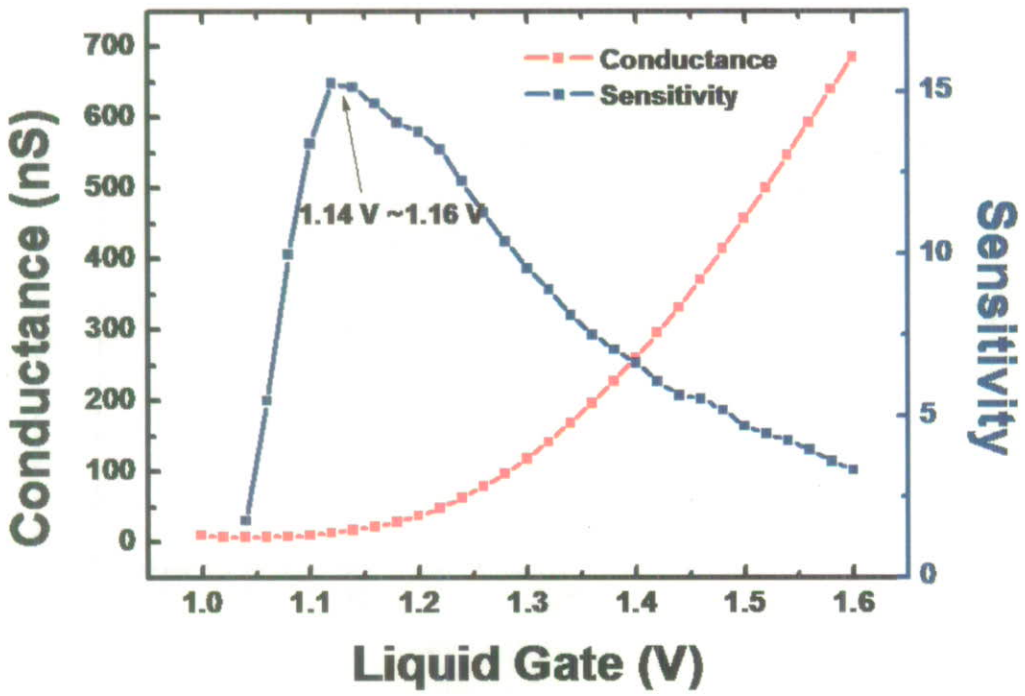

Figure 12 Conductance vs. Liquid gate plot accompany with the sensitivity variation trend.

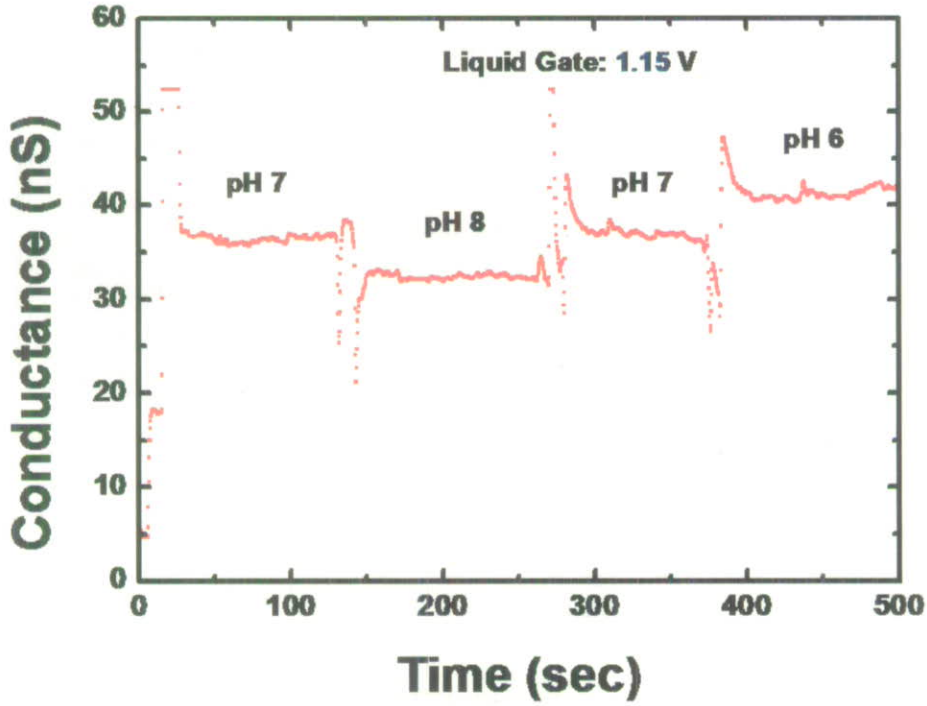

Figure 13 N-type NWFET pH sensing at fixed liquid gate (1.15V)

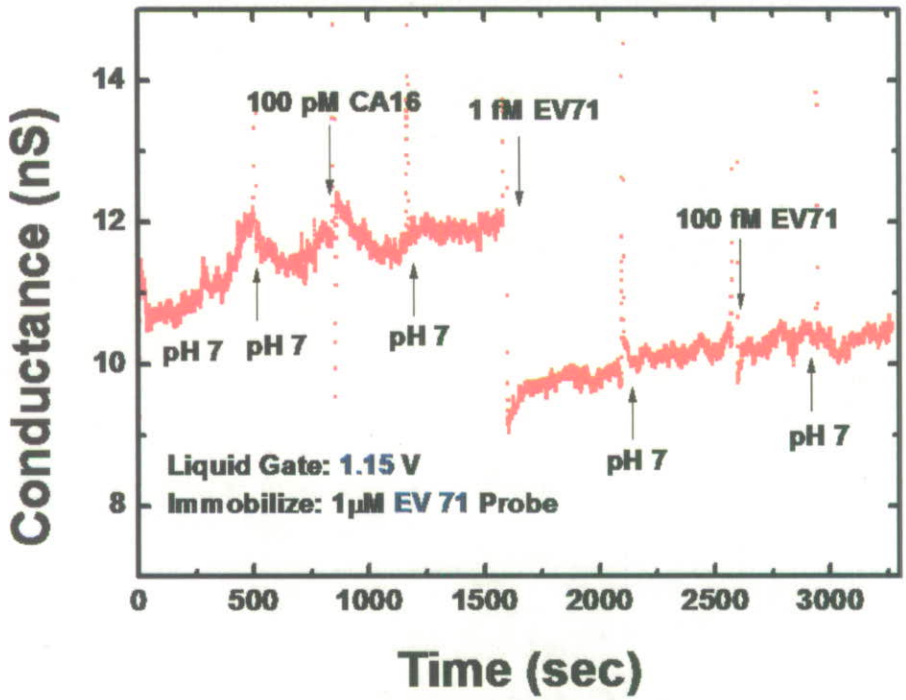

Figure 14 Real-time biosensing process of EV 71 (phosphate buffer elution between each sample in fixed flow rate: 5 ml/h).

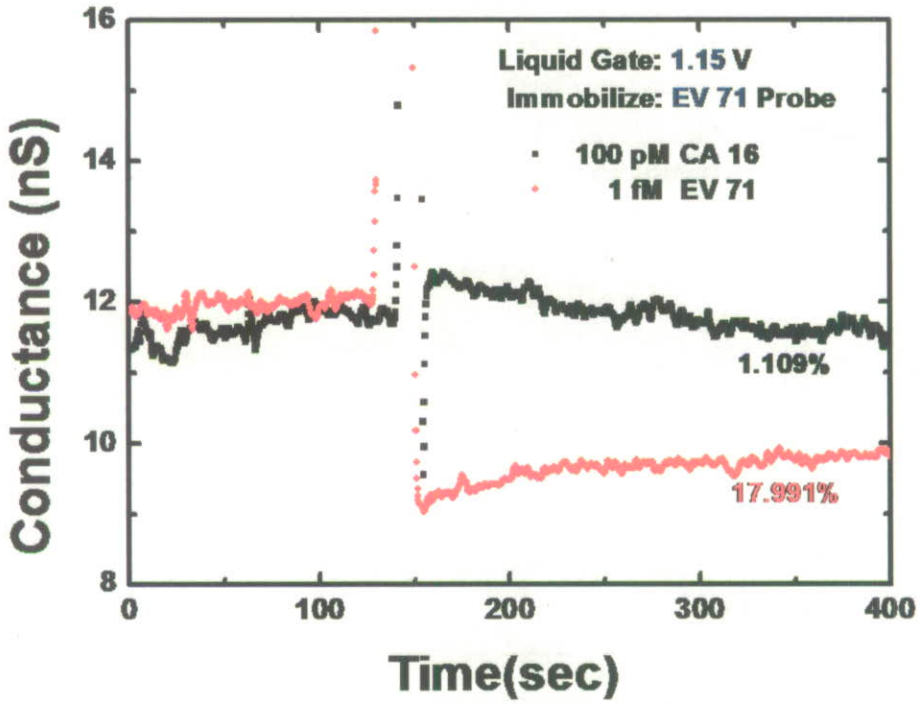

Figure 15 Compare the conductance variation rate between 10 pM CA 16 (negative control) and 1fM EV 71(experiment).

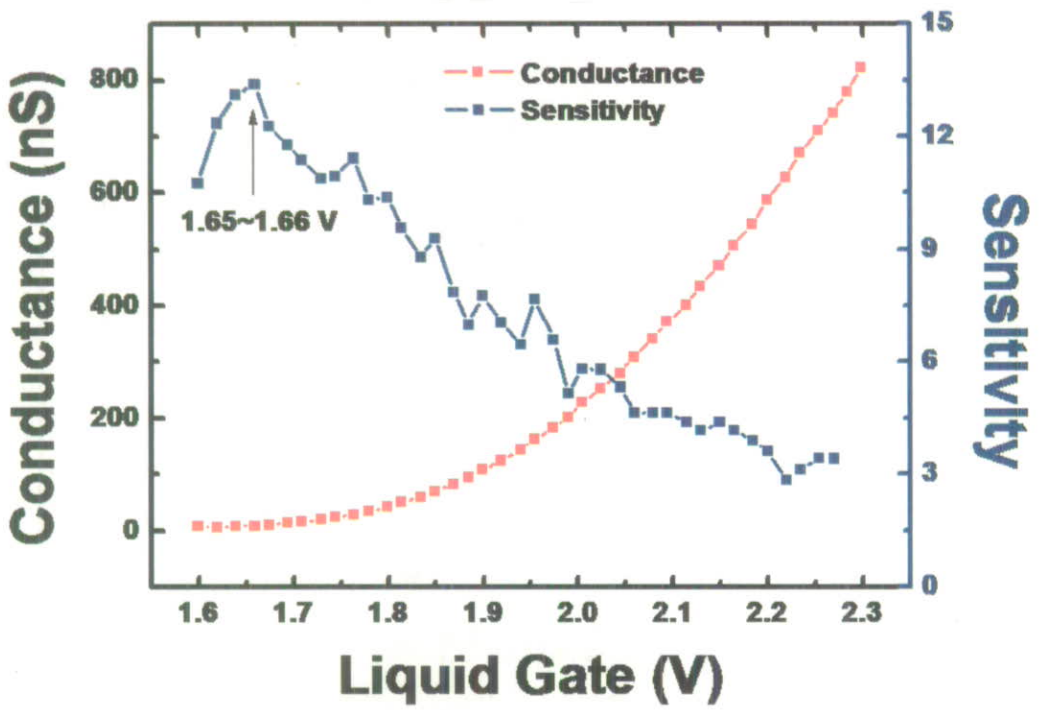

Figure 16 Conductance vs. Liquid gate plot accompany with the sensitivity factor after hot water washed

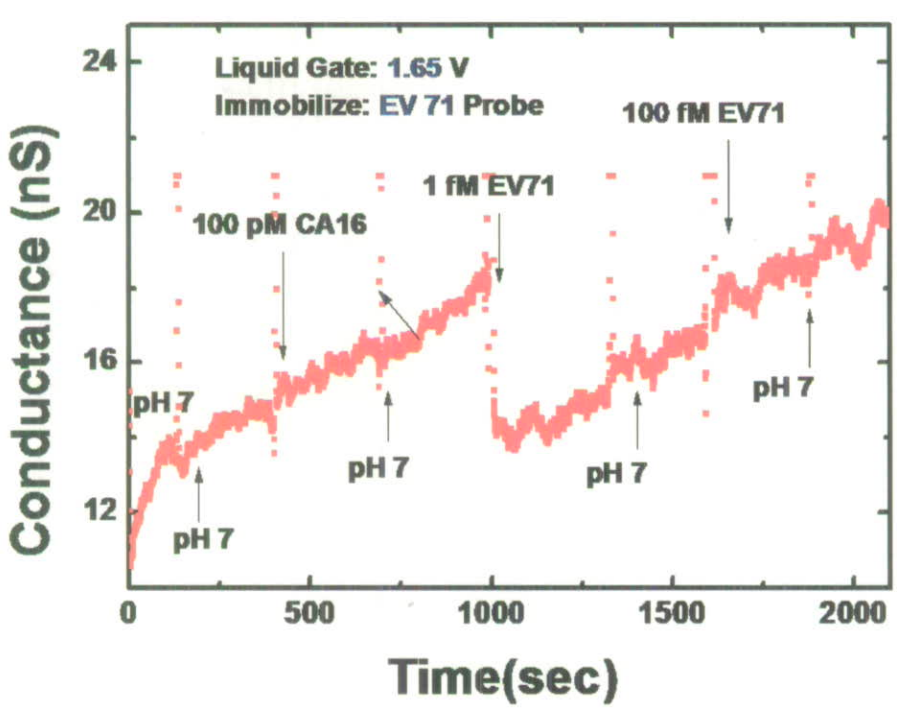

Figure 17 EV 71 biosensing process after hot water washed condition.

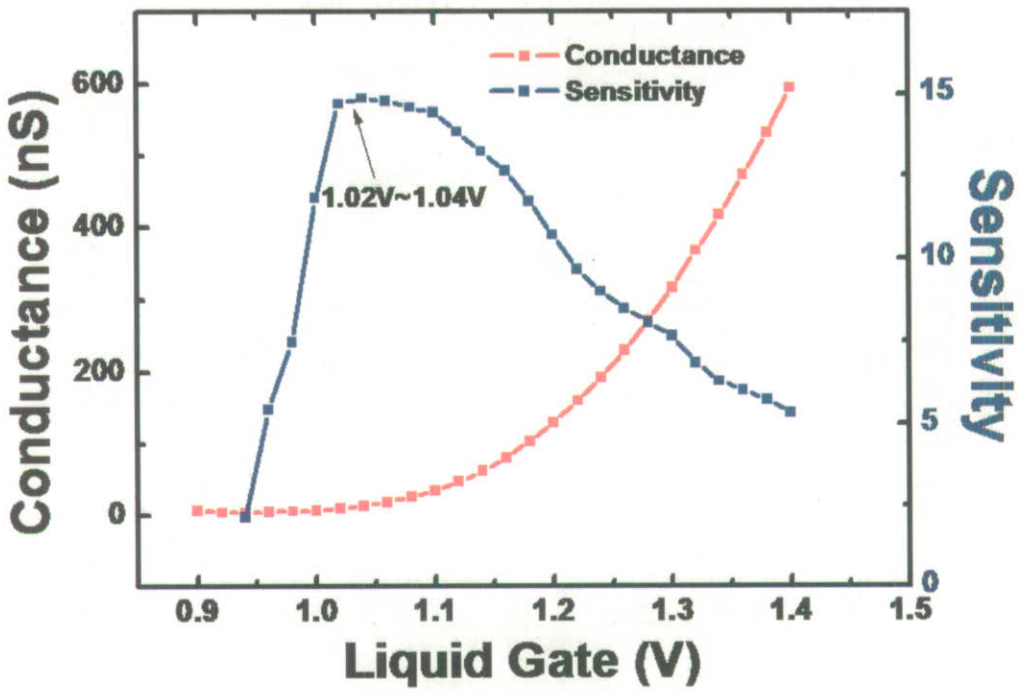

Figure 18 Calculating the most sensitive point of CA 16 biosensing

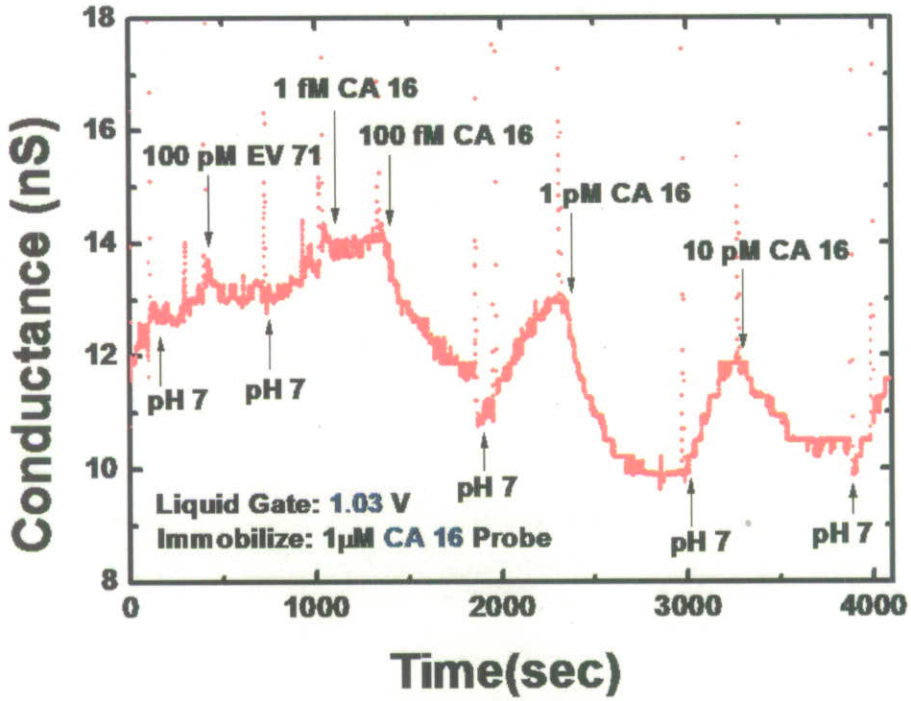

Figure 19 CA 16 Biosensing Process, the conductance value would reverse after pH 7 buffer solution flushed

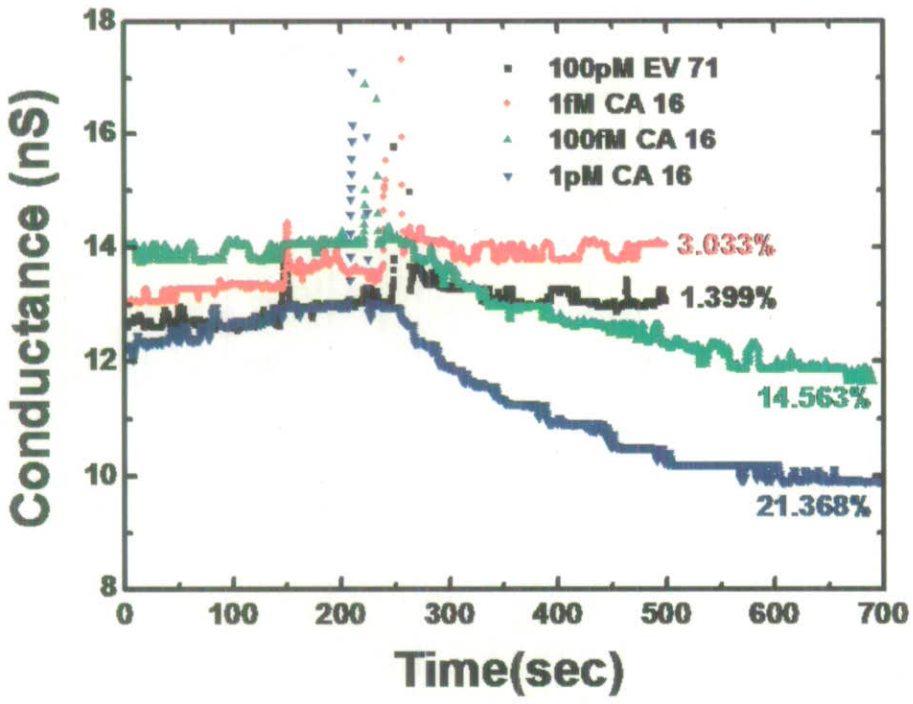

Figure 20 Comparison of different CA 16 DNA samples with control set

附錄：

(1) 計畫經費執行情形

經費項目		合計		備註
		金額	百分比(%)	
人事費		700,000	100	
業務費	研究設備費			
	材料與雜費	650,282	61.80	尚在執行中
管理費		247,825	100	

與原計畫規劃差異說明：

(2) 計畫人力執行情形

執行情形	總人力(人年)	研究員級	副研究員級	助理研究員級	助理
原訂	6	1	1	2	2
實際	6	1	1	2	2
差異	0	0	0	0	0

與原計畫規劃差異說明：

無差異